

PAPER • OPEN ACCESS

Wavelength-stabilized DBR high-power diode laser

To cite this article: R Paoletti *et al* 2020 *J. Phys. Photonics* **2** 014010

View the [article online](#) for updates and enhancements.

You may also like

- [A comparative study of thermal characteristics of GaN-based VCSELs with three different typical structures](#)
Yang Mei, Rong-Bin Xu, Huan Xu et al.
- [Design and fabrication of bi-functional TiO₂/Al₂O₃ nanolaminates with selected light extraction and reliable moisture vapor barrier performance](#)
Yalian Weng, Guixiong Chen, Xiongtu Zhou et al.
- [Improved green thermal activated delayed fluorescence OLEDs based on thermally evaporated distributed Bragg reflector \(DBR\) of MgF₂/ZnS](#)
Yanqiong Zheng, Juncong Chen, Weiguang Li et al.



PAPER

Wavelength-stabilized DBR high-power diode laser

RECEIVED

18 September 2019

REVISED

27 November 2019

ACCEPTED FOR PUBLICATION

2 January 2020


PUBLISHED

28 January 2020

Original content from this work may be used under the terms of the [Creative Commons Attribution 3.0 licence](#).

Any further distribution of this work must maintain attribution to the author(s) and the title of the work, journal citation and DOI.



R Paoletti, C Coriasso , G Meneghini, F Gaziano, P Gotta, S Codato, A Maina, G Morello, P De Melchiorre, G Pippione, E Riva, M Rosso, A Stano and M Gattiglio

Convergent Photonics—Prima Electro, Via Schiaparelli 12, 10148 TORINO Italy

E-mail: claudio.coriasso@convergent-photonics.com

Keywords: high-power diode laser, wavelength stabilization, DBR, identical layer epitaxy

Abstract

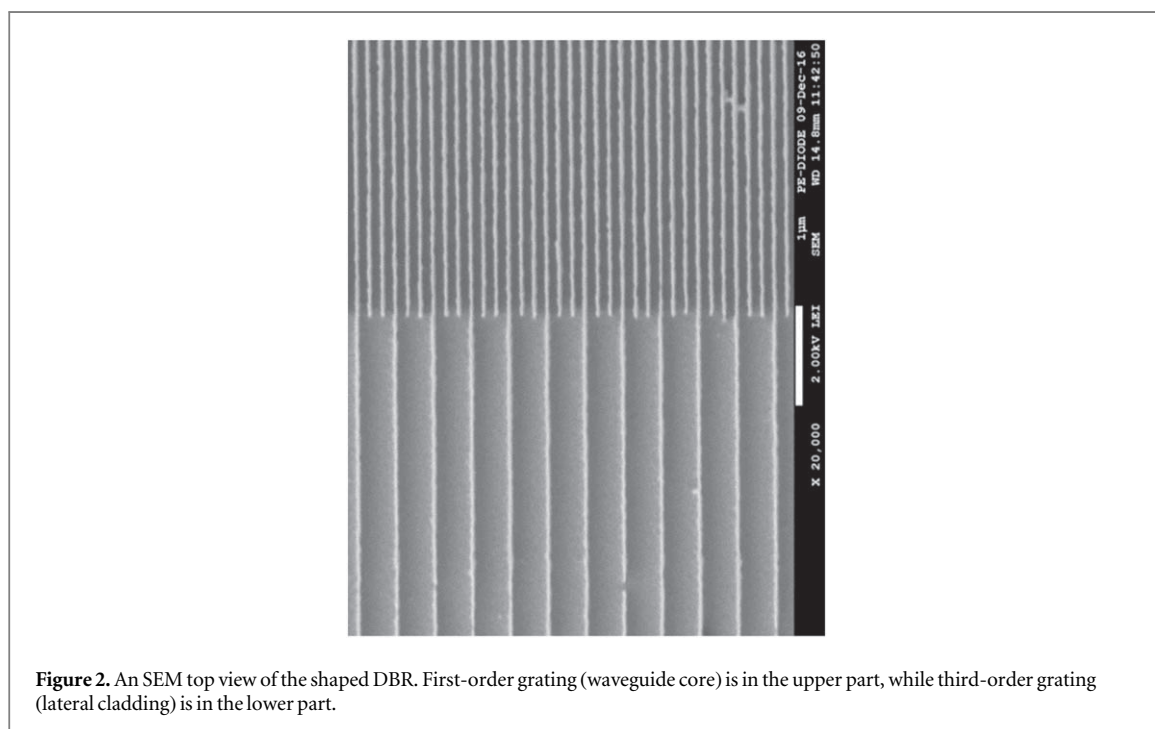
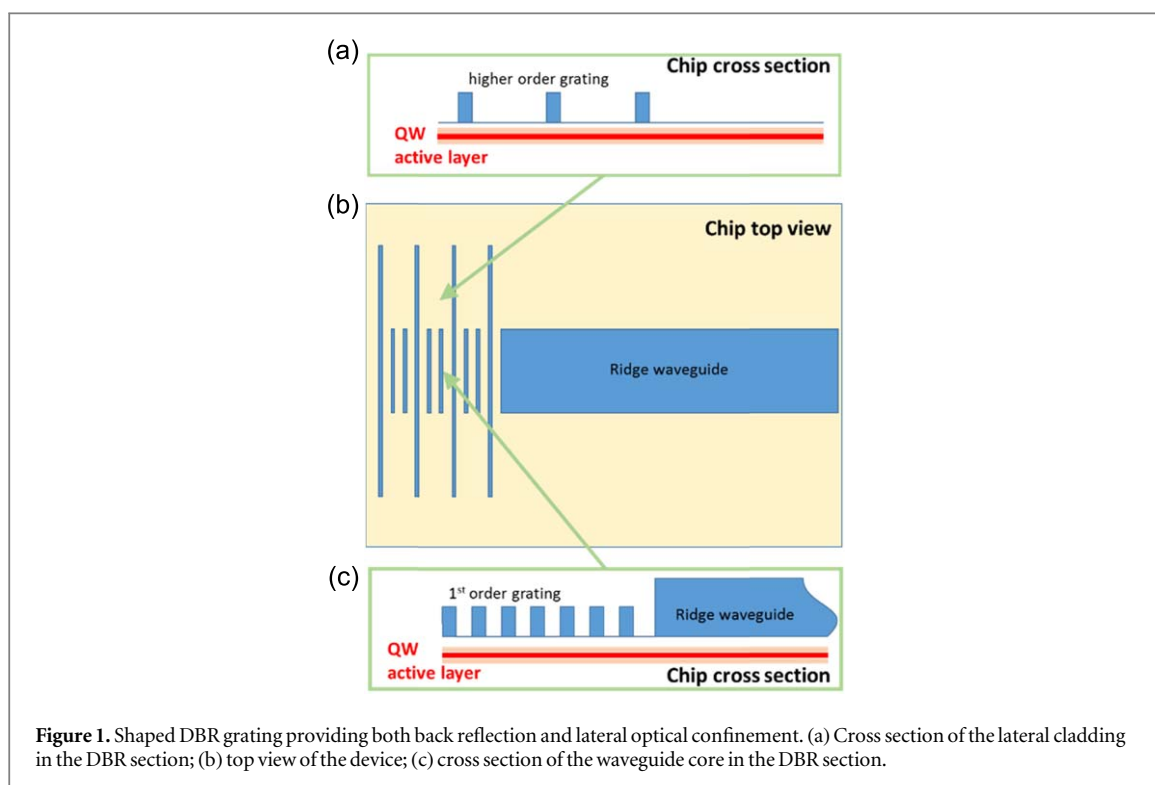
This paper reports a wavelength-stabilized high-power diode laser emitting up to 14 W CW in the 9xx nm range. Wavelength stabilization is achieved by a distributed Bragg reflector (DBR) monolithically integrated in the diode laser chip. Key features are identical layer epitaxy (ILE) and the use of a multiple-order electron beam lithography (EBL) optical confining grating. ILE avoids any regrowth or complex technology processes, while EBL multiple-order grating allows narrow-band back reflection and effective lateral optical confinement, and makes it possible to stabilize multiple wavelengths on the same wafer using a manufacturable and reliable technology. DBR diode lasers with different pitches, whose wavelengths were 3 nm spaced, were fabricated and high spectral purity (95% optical power within about 0.6 nm) and wavelength stability were measured. Moreover, the high uniformity of performances across the wafer with different emitted wavelengths demonstrates the maturity of the proposed technology for high-yield, high-volume laser diode production for wavelength-stabilized applications. A multi-emitter module, including ten DBR diode lasers, collimating and focusing optics, showed 100 W CW wavelength-stabilized output power at 14 A in a 135 μm core optical fiber within 0.17 NA. Single diode lasers, or multi-emitter modules, can be used to combine high-power optical beams by wavelength division multiplexing (WDM) using dichroic optics, scaling up beam power to the kW range and maintaining optical beam quality.

1. Introduction

Wavelength-stabilized high-power diode lasers are key components in many applications, including 976 nm optical pumping of Yb-doped fiber lasers or laser beam combining for high-power, high-radiance sources exploiting wavelength division multiplexing (WDM) [1–3].

A distributed Bragg reflector (DBR) monolithically integrated in the semiconductor diode chip is an attractive, potentially high-yield and low-cost, technology if compared with the more common hybrid coupling of volume Bragg gratings (VBG) to packaged high-power Fabry–Perot diode lasers [4]. Many demonstrations of high-power distributed feedback (DFB) and DBR diode lasers are reported in the literature [5–8]. VBG implies a considerable increase in the cost due to the need for additional components and their adjustment; moreover, it is limited by additional losses in the optical cavity, and intrinsic sensitivity to mechanical disturbances.

This paper reports a DBR high-power diode laser (DBR-HPDL), emitting up to 14 W CW (limited by thermal roll off) in the 9xx nm range. A proprietary shaped DBR [9], fabricated by electron beam lithography (EBL) and dry etching, constitutes the high-reflection mirror of the diode laser. By changing the grating pitch, multiple stabilized wavelengths on the same wafer are achievable. The shaped DBR includes gratings with different orders and different duty cycles, in the waveguiding region and in the lateral claddings; see figures 1 and 2. This allows narrow-band back reflection, as well as effective and controlled lateral optical confinement, avoiding additional modal losses in the DBR section. Moreover, the laser structure is identical (identical layer epitaxy (ILE)) in both the active section and the DBR section, avoiding regrowth or quantum well (QW) intermixing techniques which could be critical at high-power operation. The internal optical pumping induces the required transparency of the DBR section during device operation.



DBR-HPDL wafers with different grating pitches, whose wavelengths were 3 nm spaced, were fabricated. High spectral purity, see figure 3, and high wavelength stability versus injected current (wavelength shift reduced by a factor of about five compared to Fabry–Perot lasers) suggests that DBR-HPDL is a suitable device for a wavelength-stabilized pump source and high brightness.

A statistical analysis of the device's performance, including emitted wavelengths, demonstrated high uniformity across a 4" wafer, and capability analysis showed high yield for the key parameters. This analysis demonstrated the maturity of the proposed technology, shaped DBR with ILE, for high-yield highly-manufacturable wavelength-stabilized high-power diode lasers.

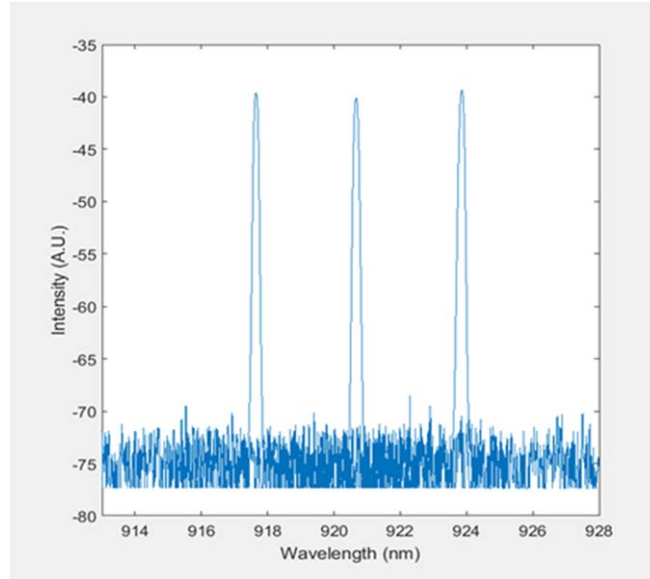


Figure 3. Superimposed spectra (10 A bias) emitted by three DBR-HPDL, obtained from the same wafer, with three different grating pitches.

A multi-emitter package, including ten DBR-HPDLs, slow-axis and fast-axis collimating lenses, mirrors and focusing lens showed a 100 W CW at 14 A wavelength-stabilized output beam in a 135 μm core optical fiber within 0.17 NA.

2. Device design

The laser epitaxial structure consists of a single 8 nm InGaAs/AlGaAs QW embedded between asymmetric graded-index separate-confinement heterostructure (GRIN-SCH) AlGaAs layers. GaAs cap, AlGaAs p cladding and AlGaAs n cladding complete the epitaxial structure; see figure 4(a).

The QW and the epitaxial layers (thickness, doping and compositions) were designed and optimized using the software Harold by Photon Design [10]. The modelling drove an extensive experimental study with successive generations of prototypes fabricated. Figure 4(b) shows the vertical refractive index profile of the epitaxial heterostructure and the vertical (fast-axis) optical mode.

Low optical propagation loss ($< 0.8 \text{ cm}^{-1}$), mainly due to free-carrier absorption control through proper layer doping and heterostructure design, allowed a 5 mm cavity length. Lateral mode confinement was provided by a 130 μm wide ridge waveguide structure whose effective index step was $\Delta n_{\text{eff}} = n_{\text{eff,core}} - n_{\text{eff,clad}} \cong 1 \times 10^{-3}$, where $n_{\text{eff,core}}$ and $n_{\text{eff,clad}}$ are the effective indexes in the core and cladding regions, respectively. A DBR was integrated on the rear facet side, providing a reflectance of about 90%, replacing the standard (for Fabry–Perot lasers) high-reflectance coating.

Figure 5 shows the calculated spectral reflectance of the DBR section, and figure 6 shows a calculation of the fabrication tolerance as a function of the grating shape parameters. These calculations were performed using a 1D transfer-matrix modelling tool in the effective index approximation. Despite the apparent critical time control of the grating etching, the wide process window allowed by this design resulted in a high fabrication yield.

The broad-area asymmetric GRIN-SCH structure allowed reduced vertical \perp and lateral \parallel far-field, (less than $57^\circ \perp \times 12^\circ \parallel$, full width@1/e²). High slope efficiency ($> 1 \text{ A W}^{-1}$), low series resistance ($< 20 \text{ m}\Omega$) and high wall-plug efficiency ($> 60\%$) were also demonstrated. To achieve a high reflectance in a relatively short length, the DBR grating has to be deeply etched, starting from the top of the ridge [5]. In our device, the cumbersome deep etch was avoided, and the technological process was significantly simplified through the introduction of the shallow etched shaped DBR.

The shaped DBR was fabricated by EBL in a planar region corresponding to the bottom of the ridge; see the schematic diagram in figure 7. The lateral grating, with a lower effective refractive index, acts as an optical cladding providing a lateral optical confinement of the beam; see figure 8. Effective refractive indexes, shown in figure 8, were calculated by solving the Helmholtz equation for the vertical refractive index profile in the two regions.

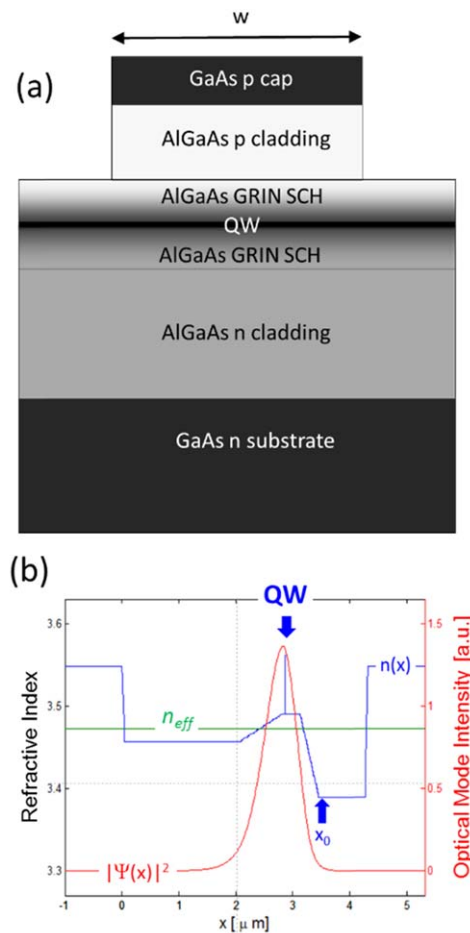


Figure 4. (a) A schematic cross section of the diode laser heterostructure showing the ridge width, w . (b) The vertical refractive index profile $n(x)$ and optical mode $|\Psi(x)|^2$. The active layer (QW) position and the effective refractive index n_{eff} are shown.

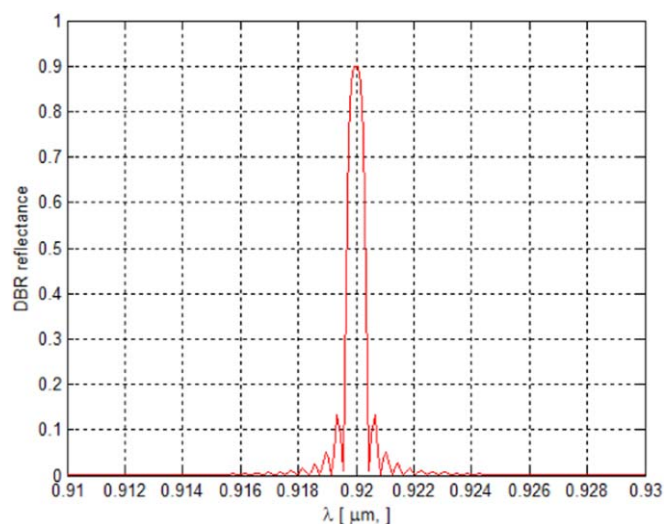


Figure 5. Calculation of the DBR spectral reflectance for a 0.5 mm long first-order grating.

Ideally, the lateral confinement could be simply achieved by omitting the lateral grating. However, the EBL writing in wider areas and the loading effect in the semiconductor etching [11] would cause a more complicated and less controllable technological process. Calculations based on the 1D transfer-matrix method, in the effective index approximation, showed that the optical lateral confinement achievable with a reduced-duty-cycle and higher-order grating can be similar to that achieved by standard ridge etching on broad-area waveguides

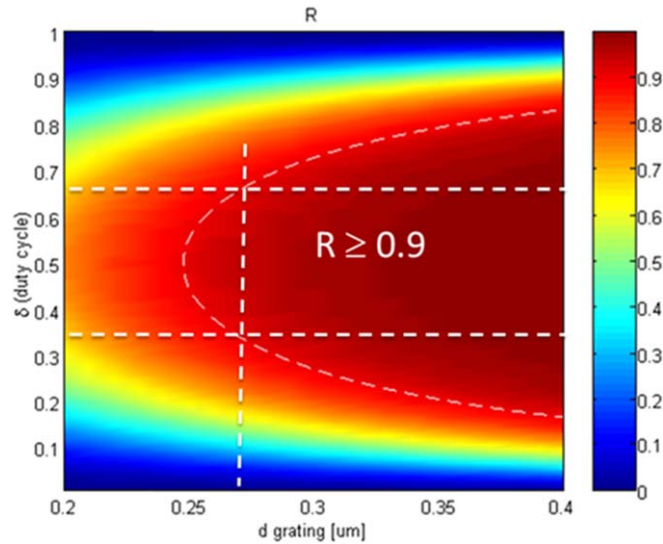


Figure 6. Process tolerance: calculation of the DBR peak reflectance as a function of the grating duty cycle and depth (0.5 mm long first-order grating).

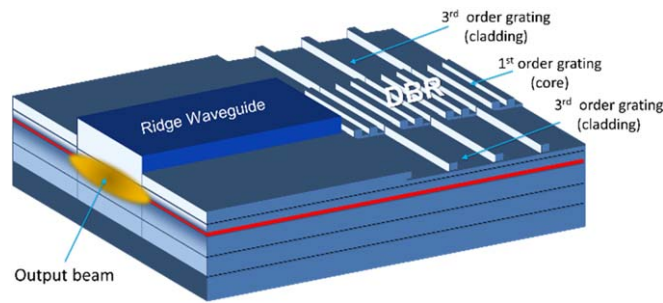


Figure 7. A schematic structure of the DBR-HPDL.

$\left(\frac{\Delta n_{eff}}{n_{eff,core}} \cong 10^{-4} \div 10^{-3}\right)$ and finely tuned by changing the grating structure parameters (grating order, duty cycle, etching depth); see figure 9.

Conventional technology for the DBR section, which needs to be transparent at the wavelength emission of the laser diode, uses a higher-energy-gap material: butt-coupling or QW intermixing techniques are the most widely used technology approaches. However, avoiding epitaxial regrowth or high-temperature annealing in high-power laser diodes is of utmost importance for the reduction of extremely critical defects within the active cavity. Moreover, both techniques would imply a significant manufacturing cost increase.

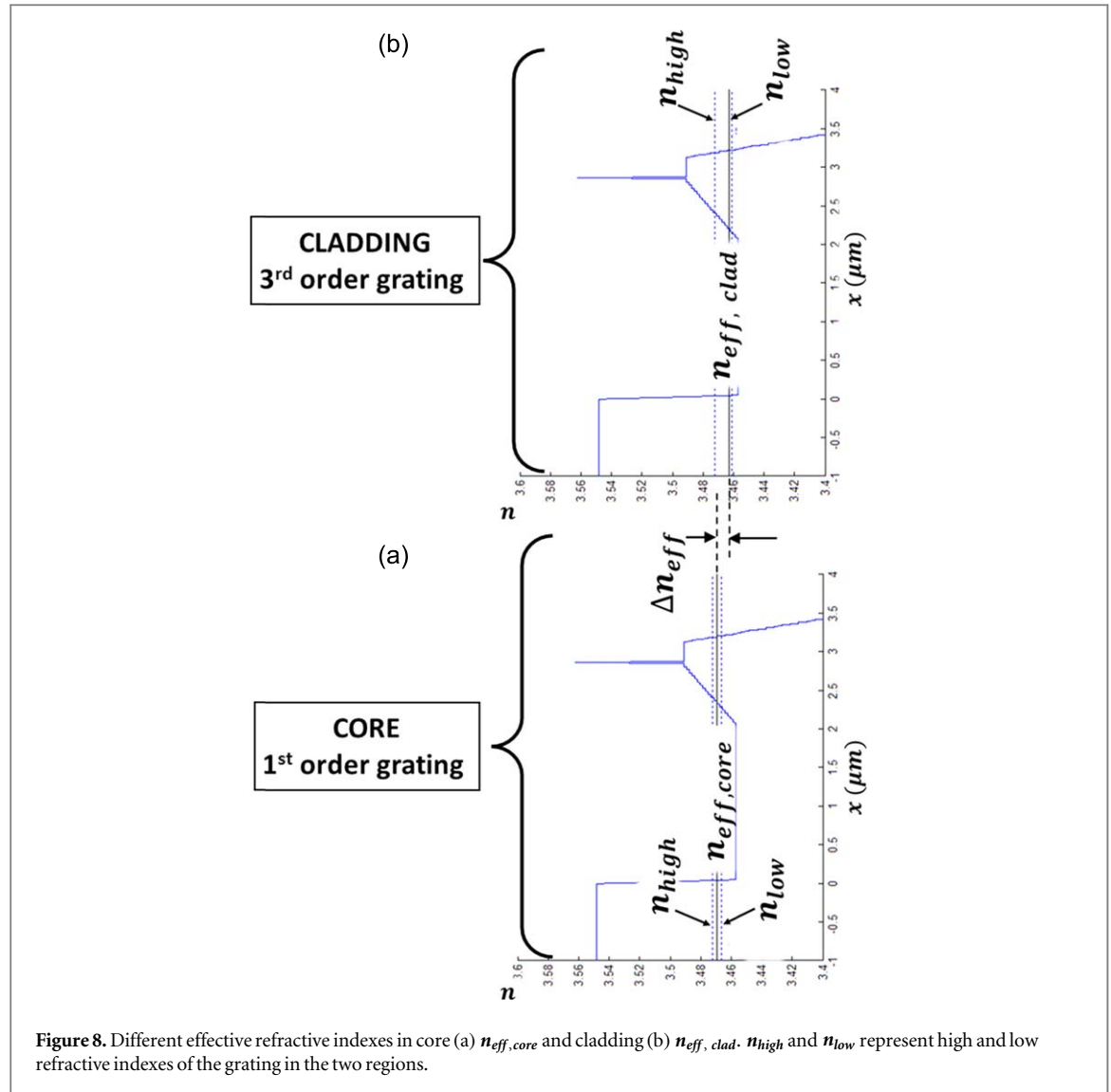
Due to the high optical power density within the laser cavity, none of the above techniques were required in our device. Indeed, the optical beam induces the required transparency in the DBR section, according to modelling results achieved by an iterative numerical tool integrating a 1D transfer-matrix, laser rate equations and nonlinear optical properties of the QW, see figure 10. The insertion loss penalty due to the residual absorption in the DBR section produces a negligible effect, in the very few percent range, on the laser threshold and slope efficiency.

The simplified manufacturing process advantage significantly overcomes this small penalty, which in any case does not prevent reaching the optical power target.

3. Device fabrication

The InGaAs/AlGaAs/GaAs epitaxial heterostructure was grown by metal organic chemical vapor deposition on an n-doped (100) 2-degree-off 4" GaAs substrate.

Here, 130 μm wide broad-area ridge waveguides together with planar regions at the ridge bottom, corresponding to DBR sections, were fabricated by wet chemical etching; see figure 11(a). Then, the 500 μm long shaped gratings,



forming the DBR sections, were fabricated by EBL in the planar regions; see figure 11(b). The adopted solution implies a single etching process for the whole DBR section, which at the same time provides high reflectance and lateral optical confinement. The resulting technological fabrication process is significantly simplified.

Different grating pitches can be written in different devices of the same wafer, thus allowing the fabrication of DBR-HPDLs emitting at different wavelengths.

We fabricated DBR-HPDLs with three different grating pitches corresponding to three emitted wavelengths spaced by 3 nm on the same 4" wafer.

The technological fabrication process for the DBR section, depicted in figure 12, starts with a 200 nm resist layer placed on the whole 4" wafer with ridges and planar regions already defined; see figure 12(a). After baking, the resist is directly written with an E-beam; see figure 12(b). The grating pattern is automatically divided in fields and properly aligned to the ridge by marker recognition. The grating pitch is finely tuned by the field size definition (around $700 \mu\text{m}^2$). The single grating area is smaller than the field, thus stitching errors between fields are avoided.

The E-beam-written resist is then developed and removed up to the semiconductor surface, figure 12(c). Then, a reactive ion etching–inductively coupled plasma with an $\text{Ar}:\text{Cl}_2:\text{CH}_4$ gas mixture transfers the DBR geometry to the semiconductor material by deep etching; see figure 12(d).

Following RIE plasma cleaning of the surface from resist residuals, figure 12(e), a passivation SiN layer is deposited using the plasma-enhanced chemical vapor deposition technique; see figure 12(f).

The wafer process is then completed by contact window definition on the p side, p-metallization, wafer thinning and n-metallization.

SEM cross sections of fabricated first-order and third-order gratings are shown in figure 13. Good grating shape has been demonstrated since the optimized writing/etching technological process.

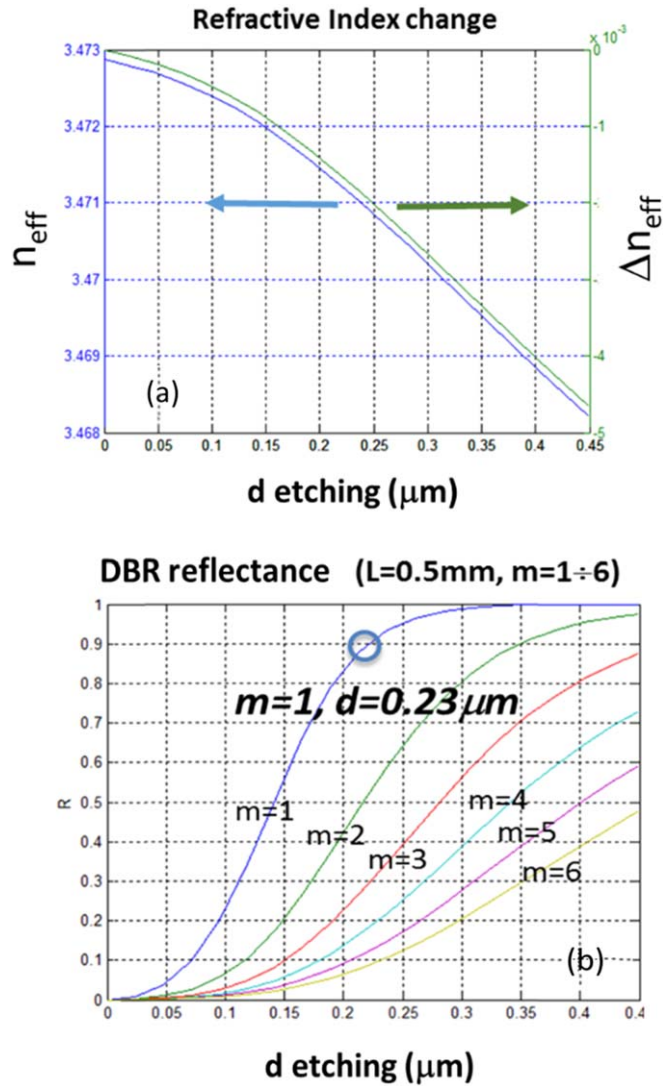


Figure 9. Calculation of the optical confinement (a) and of the DBR reflectance at the Bragg wavelength (b) as a function of the etching thickness, at different grating orders, m .

A low reflectance mirror coating of about 2% is deposited on both laser facets after bar scribing, and a proprietary passivation technology is used together with an unpumped current blocking region of $300 \mu\text{m}$ close to the front laser facet to increase the catastrophic optical mirror damage (COMD) threshold and enable reliable operation at high power. The total length of the fabricated DBR-HPDL is 5.5 mm, including a 5.0 mm long active section and a 0.5 mm long DBR section.

4. Experimental results

A 4" wafer, integrating three different pitches, whose wavelengths were spaced by 3 nm, was processed and tested, demonstrating the maturity of the technology from the statistical data of the main functional characteristics.

Bars with different grating pitches were tested in pulsed conditions ($\tau = 3 \mu\text{s}$ pulse duration, $\delta = 0.1\%$ duty cycle) by a semi-automatic measurement setup, to derive electro-optical characteristics across the wafer and for different grating pitches. The goal was to analyse the variability of shaped grating technology across the wafer and to verify the uniformity of performances at different wavelengths.

Figure 14 shows statistical distribution of the threshold current and slope efficiency versus the grating pitch, as a key indicator of device performance. Box plots show 25%-75% population for the three different pitches: very limited variation of the threshold can be identified, mainly due to the gain peak—Bragg wavelength detuning, and consequently slightly different threshold gain conditions for the three pitches. Good and uniform slope efficiency, close to 1 W A^{-1} , has been obtained for the three pitches.

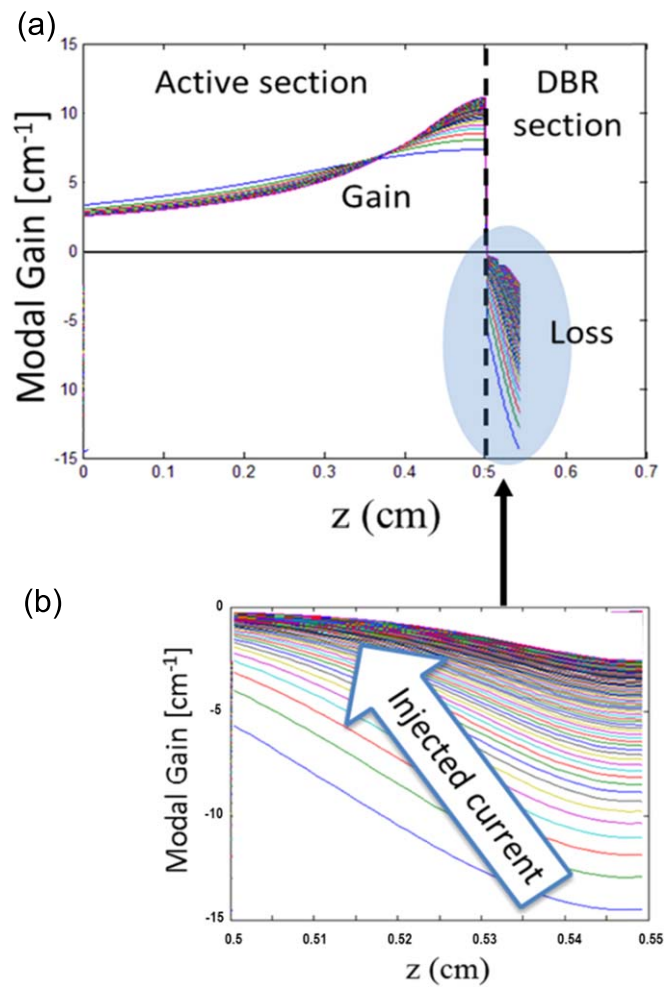


Figure 10. Calculation of the induced transparency in the DBR section as a function of the injected current into the active region from 0.5 A to 15 A, corresponding to optical power from 0 to about 14 W. (a) Whole device including active section and DBR section; (b) magnification of the DBR section.

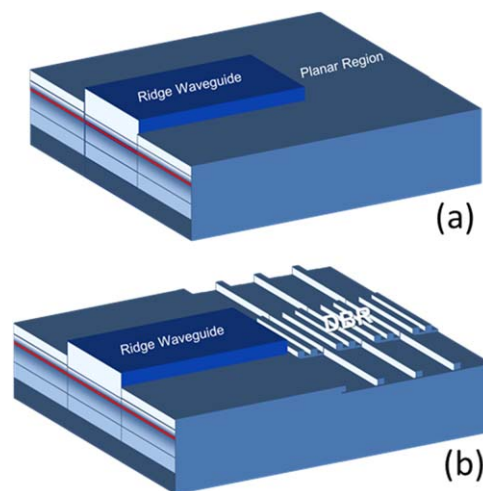
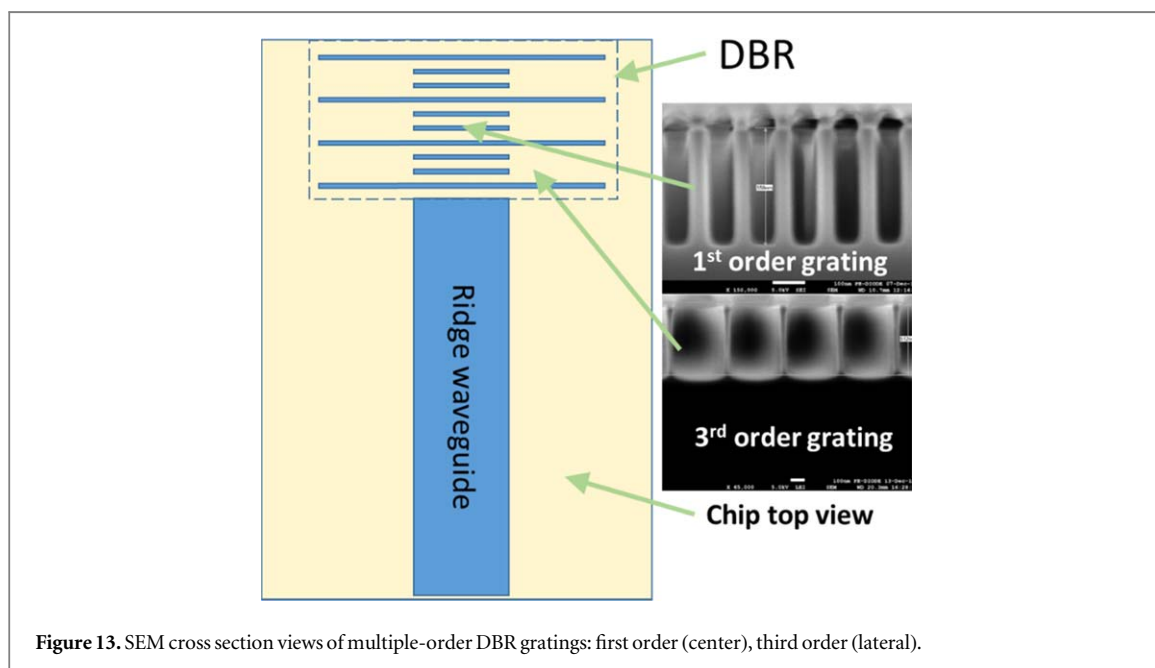
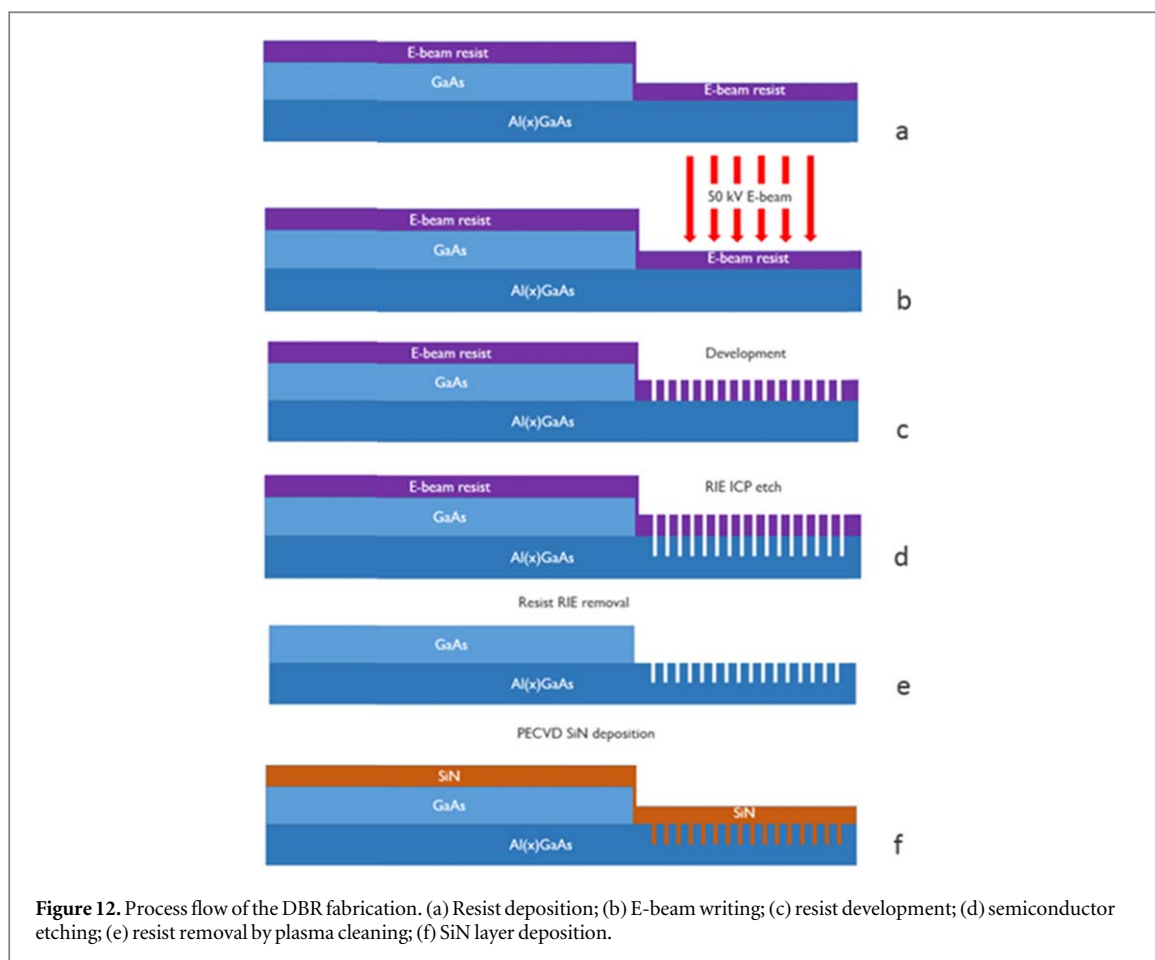


Figure 11. The device geometry before (a) and after (b) the DBR fabrication.

A set of single DBR-HPDLs have also been assembled p side down on ceramic carriers (by gold–tin hard soldering die attach), obtaining the so-called Chip on Carrier (CoC), necessary for CW tests under high bias—high-power conditions.



Low thermal resistance is necessary to ensure low junction temperature at operating conditions, critical to reduce power roll off at high current, and enhance long-term reliability. To this purpose a copper plated ceramic carrier was properly designed and used for high-power applications, ensuring a thermal resistance of the complete structure (from the active junction to the base of the carrier) in the order of $1.5\text{--}2.0\text{ K W}^{-1}$.

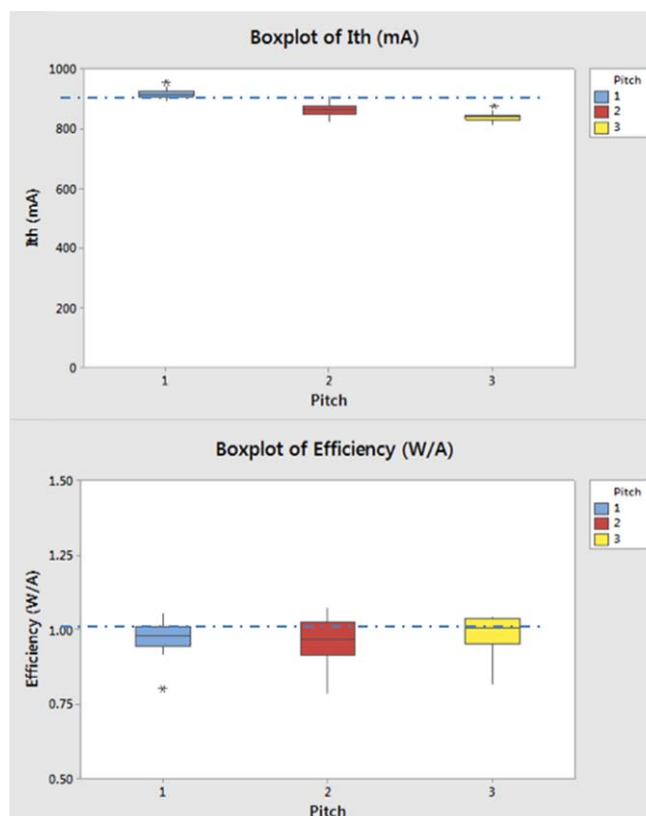


Figure 14. Box plot representation of the threshold current (*top*) and slope efficiency (*bottom*) statistics.

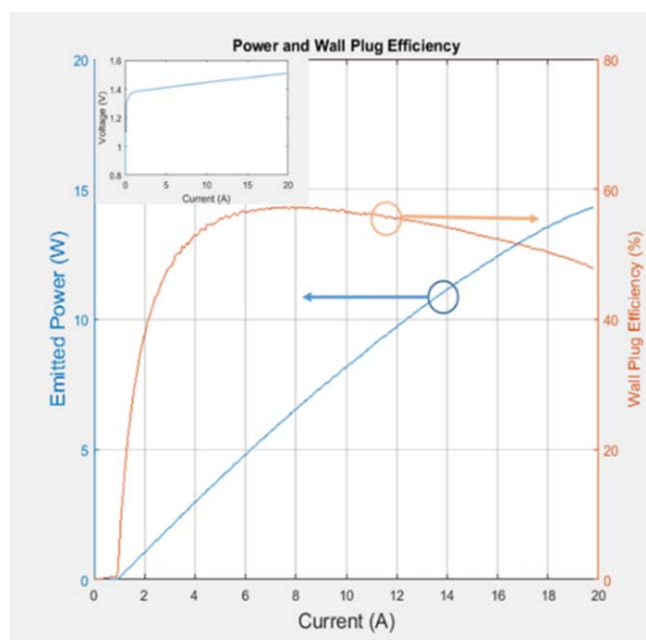


Figure 15. CW emitted power and wall-plug efficiency (diode voltage in the inset) versus injected current (measured at 25 °C).

Measurements performed in CW 25 °C on CoC demonstrated power in excess of 14 W; see figure 15.

Due to epitaxial structure design and fabrication technology a low diode voltage was achieved (about 1.5 V at 20 A), ensuring low power dissipation, decreasing the active junction temperature and strongly contributing to the long-term reliability under operating conditions.

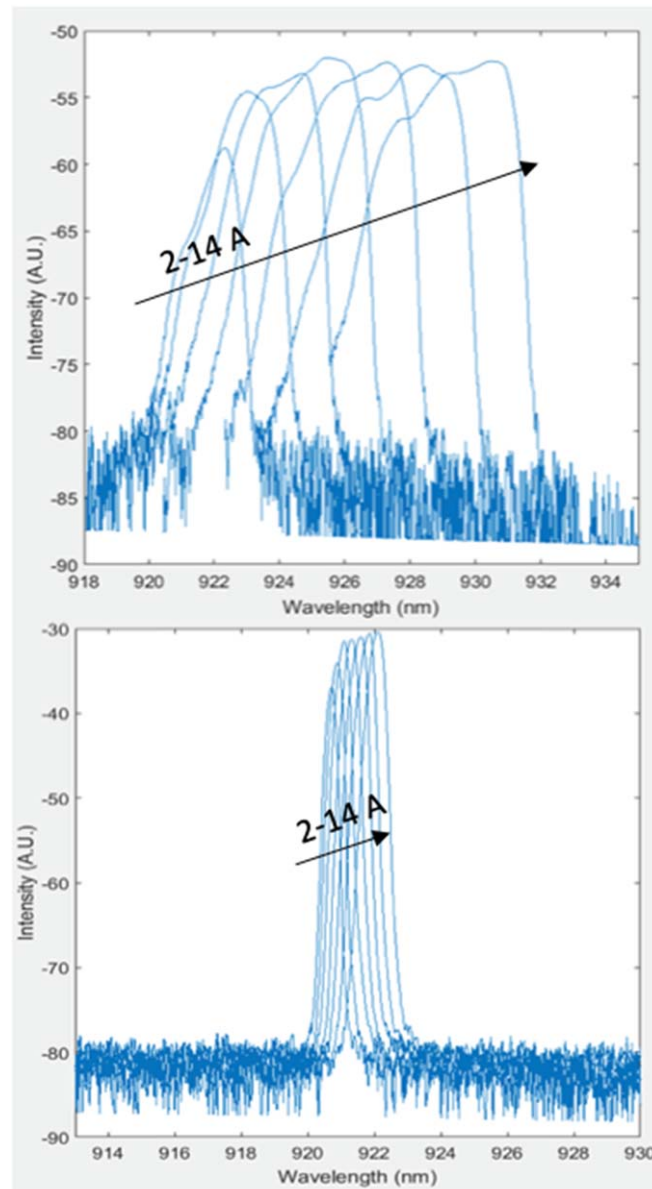


Figure 16. The emitted spectrum at 25 °C 2–14 A CW bias from the standard broad-area Fabry–Perot laser (*top*) and DBR-HPDL (*bottom*).

A high-purity emitted spectrum and good stability over the current are key requirements for a DBR-HPDL. Figure 16 shows the results of the emitted spectrum stability versus the bias current in the range of 2 to 14 A. Standard broad-area Fabry–Perot lasers usually show more than 10 nm of spectrum occupation, while the DBR-HPDL has demonstrated a reduction to less than 2 nm, in the same bias range.

As already described, the DBR-HPDL narrow spectrum enables the possibility of multiple emitted wavelengths from the same wafer, by writing multiple pitches. The results of devices with the three different pitches, mentioned in section 3, are reported in figure 3. Three emitted wavelengths, 3 nm spaced, were obtained with similar characteristics of emitted power and spectral width.

Having analysed the key parameter statistics and defined preliminary device specifications—and therefore production test limits—for a typical high-power laser diode application, it was possible to study the process capability, thus the manufacturability of this technology. A preliminary study was based on the slope efficiency as the key performance indicator. Figure 17 shows the overall distribution and capability analysis for the slope efficiency parameter: a production yield of 98% was demonstrated, for a lower production test limit (LSL) of 0.8 W A^{-1} . More accurate capability analysis will imply a precise definition of the product specifications based on the power required for the specific application; however, the tight distribution is a promising indicator of the maturity of the present technology.

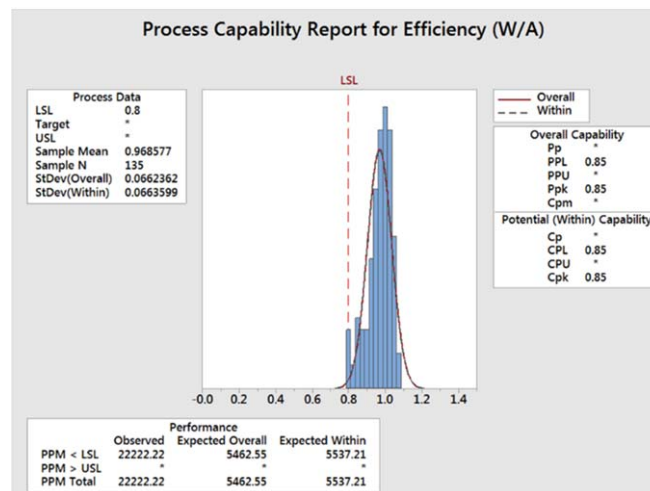


Figure 17. Capability analysis of slope efficiency, showing 98% yield.

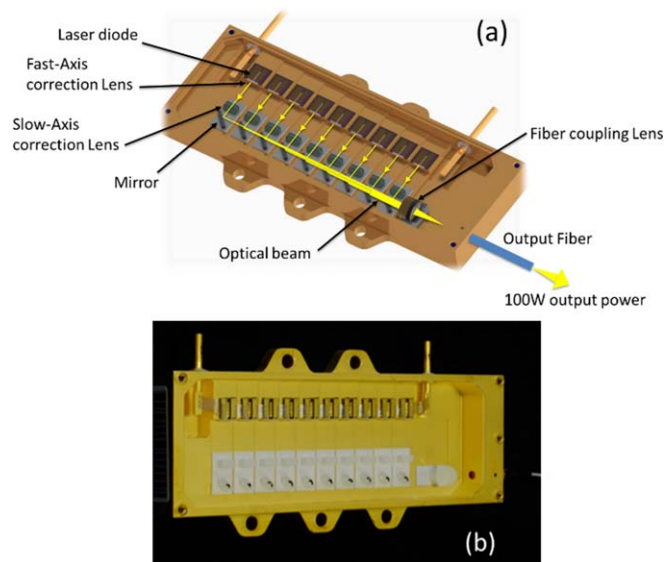


Figure 18. The 100 W multi-emitter module with ten DBR-HPDLs on a stair package: (a) a schematic diagram, and (b) a picture of the fabricated module.

Device manufacturability enabled the use of the DBR-HPDL in the standard production line assembly of high-power multi-emitter modules. Ten DBR-HPDLs were assembled into a module, where their beams are spatially multiplexed by collimating lenses and mirrors; see the schematic diagram in figure 18(a). Each single beam is collimated using a fast-axis collimating (FAC) lens for the vertical divergence, and a slow-axis collimating (SAC) lens for the lateral divergence. The collimated beams are then routed by 45° micro-mirrors toward a common fiber lens which focuses all of them into the output fiber core. Each DBR-HPDL, including its FAC, SAC and mirror, is mounted on a different step of a stair fabricated in the module package, thus allowing the different beams to be displaced to each other until the focusing lens.

The spatial multiplexing technique is intrinsically incoherent, and the output multiplexed beam quality is worsened compared to single DBR-HPDL beams. In particular, the output beam product parameter (BPP) increases by a factor of about ten; it is still within the beam quality requirement for optical pumping of an Yb-doped fiber laser.

Fabricated multi-emitter modules, figure 18(b), showed typical characteristics of 100 W CW and 0.6 nm spectral width, with 95% of power in 0.17 NA within a $135\ \mu\text{m}$ core/ $155\ \mu\text{m}$ cladding optical fiber; see figure 19.

Fabricating different multi-emitter modules with a set of DBR-HPDLs emitting at different wavelengths would allow a spectral combination of their output beams to preserve the BPP, thus increasing the brightness of the total combined output beam [1].

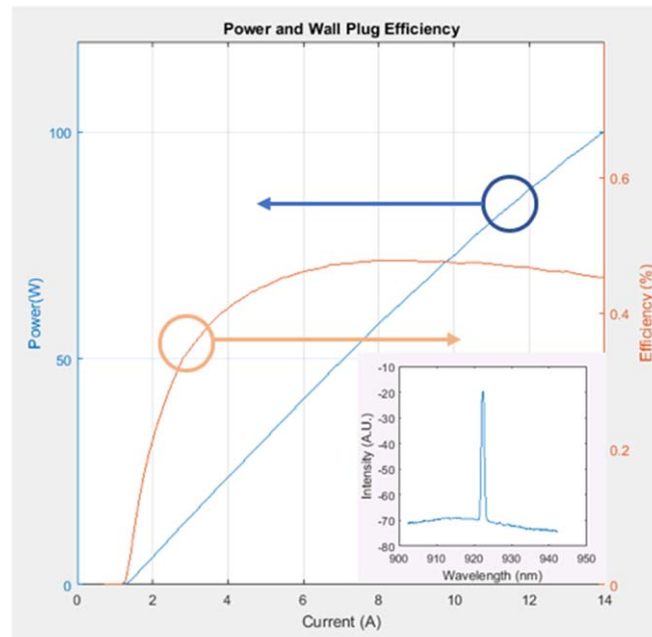


Figure 19. CW emitted power and slope efficiency versus injected current (25 °C); the inset shows the emitted spectrum.

5. Conclusions

DBR-HPDLs exploiting multiple-order EBL optical confining gratings have been demonstrated using InGaAs/AlGaAs/GaAs ILE material. The fabricated devices emitted up to 14 W CW in the 920 nm range, and demonstrated high spectral purity and wavelength stability versus the injected current. EBL grating technology enables a multi-wavelength array of diode lasers simply by varying grating pitches along the wafer.

This work demonstrates DBR-HPDLs fabricated on the same 4" wafer, with emitted wavelengths spaced by 3 nm and similar electro-optical characteristics. Performance uniformity across the wafer, as well as across different grating pitches, is a key indicator of a manufacturable and reliable technology. It suggests DBR-HPDL as a suitable device for a wavelength-stabilized pump source and high brightness applications exploiting WDM for high-power laser beam combining. A multi-emitter module including ten spatially multiplexed DBR-HPDLs showed 100 W CW output optical power in a 135 μm core fiber within 0.17 NA.

Acknowledgments

We acknowledge significant contributions to device fabrication and DBR modelling from Guido Roggero and Matteo Manachino in the early stage of the device development.

ORCID iDs

C Coriasso  <https://orcid.org/0000-0002-2916-6376>

References

- [1] Fan T Y 2005 *IEEE J. Sel. Topics Quant. Electron* **11** 567
- [2] Sverdlov B, Mohrdiek S, Pawlik S, Matuschk N and Lichtenstein N 2008 *Proc. SPIE* **6876** 68761H
- [3] Laukart A, Kohl S, Fritsche H, Grohe A, Kruschke B and Schmidt M 2016 *Phys. Procedia* **83** 1397
- [4] Fritsche H, Koch R, Krusche B, Ferrario F, Grohe A, Pflueger S and Gries W 2014 *Proc. SPIE* **9134** 91340U
- [5] Crump P, Fricke J, Schultz C M, Wenzel H, Knigge S, Brox O, Maaßdorf A, Bugge F and Erbert G 2012 *Proc. SPIE* **8241** 82410U
- [6] Kanskar M, He Y, Cai J, Galstad C, Macomber S, Stiers E, Tatavarti-Bharatarm S-R, Botez D and Mawst L 2006 *Electron. Lett.* **42** 14455
- [7] Fricke J, Wenzel H, Matalla M and Erbert G 2005 *Semicond. Sci. Technol* **20** 1149
- [8] Paoletti R et al 2018 *Proc. SPIE* **10514** 105140V
- [9] Coriasso C, Meneghini G and Paoletti R 2019 *US Patent Pending* 2019/0036306 A1
- [10] HAROLD, a heterostructure laser-diode model from Photon Design Ltd, Oxford, UK (photonond.com/products/harold.htm)
- [11] Lauvernier D, Garidel S, Legrand C and Vilmot J-P 1992 *Microelectron. Eng.* **17** 345